Functional succession of actively growing soil microorganisms during rewetting is shaped by precipitation history

Ella T. Sieradzki[1], Alex Greenlon[1], Alexa M. Nicolas[2], Mary K. Firestone[1], Jennifer Pett-Ridge[3,4], Steven J. Blazewicz[3*], Jillian F. Banfield[1,5-7*]

1 University of California Berkeley, Department of Environmental Science, Policy and Management, Berkeley CA

2 University of California Berkeley, Department of plant and microbial biology, CA, USA

3 Physical and Life Sciences Directorate, Lawrence Livermore National Laboratory, Livermore, California, USA

4 Life & Environmental Sciences Department, University of California Merced, Merced, CA, USA

5 Department of Earth and Planetary Science, University of California, Berkeley, CA, USA

6 Earth Sciences Division, Lawrence Berkeley National Laboratory, Berkeley, CA, USA

7 Chan Zuckerberg Biohub, San Francisco, CA, USA

* Corresponding authors: blazewicz1@llnl.gov and jbanfield@berkeley.edu

Competing interest statement: the authors declare no competing interests.

Keywords: soil wet-up, soil rewetting, stable isotope probing, ecophysiology, environmental microbiology, microbial ecology, metagenomics, annual grassland

Abstract

Rewetting of seasonally dry soils induces a burst of microbial activity and carbon mineralization that changes nutrient availability and leads to succession. Yet the microbial functions that underpin this succession are not well described. Further, it's unclear how previous precipitation frames microbial capacities after rewetting and how long these effects persist. We used isotopically-labeled water to rewet seasonally dry annual grassland soil that experienced either mean annual or reduced precipitation during the previous two years, and sampled at five subsequent time points. We used quantitative stable isotope probing (qSIP)-informed genome-resolved metagenomics to identify growing microorganisms, predict their capabilities, and analyze how these traits differed over time and between precipitation treatments. Organisms that grew after wetup were more abundant than non-growing organisms prior to the wet-up, suggesting that traits that initiate succession are pre-defined at the end of the prior plant growing season or via survival over the summer. Fast-growing organisms had fewer carbohydrate active enzyme (CAZy) genes per genome than slower-growing organisms, suggesting that although fast-growers were capable of degrading complex C, they may not specialize in this process. Differential abundance of CAZy genes in growing organisms throughout the succession implies that substrate availability varied with time. In contrast, the abundance of peptidases in growing organisms differed between precipitation treatments, but not over time following wet-up. Before wet-up, the soil organisms' gene inventories were different between the two precipitation treatments. Surprisingly, this legacy effect waned after

just one week. Thus, pre-wetup differences in microbial functional capacity converged shortly after rewetting.

Introduction

Following the dry season in arid and semi-arid climates, soil rewetting is a key event that triggers microbial community restructuring and substantial carbon turnover [1, 2]. This sudden increase in soil moisture has a disproportionate influence on the annual carbon budget [3] and leads to an immediate release of carbon dioxide, termed the “Birch effect”, which can arise from both abiotic and biotic processes [4–6], with biotic processes dominant in non-carbonate-rich soils [2]. Rewetting causes rapid habitat changes and a large microbial response to the altered soil environment within the span of hours: from survival and dormancy, to rapid osmotic changes and cell lysis, to peak activity [7]. These changes parallel a rapid community succession, with high rates of both growth and mortality that vary by taxonomic group [8]. While the identities of the bacterial and archaeal taxonomic groups that respond to rewetting have been described, the physiological traits that underpin organism interactions and enable rapid microbial growth and turnover following wet-up are poorly understood.

Prior research has investigated the organic resources that drive the pulse of biogeochemical processing in Mediterranean-climate grassland soils following the first autumn rain event. In addition to dry plant detritus, labile carbon and nitrogen accumulate over the summer dry season [9], largely due to low microbial metabolic rates and reduced microbial uptake [10].

66 Sustained activity of secreted extracellular enzymes [10, 11], osmotic shock [12] and secretion
67 of compatible solutes also contribute to the buildup of labile C and N pools [13–15]. Soil
68 rewetting is generally followed by high degradation rates of these substrates [16], supporting
69 initially fast-growing organisms [17]. The existing paradigm suggests these fast growers rely on
70 labile resources. However, we know little about the metabolic characteristics of the initially
71 fast-growing organisms [8] which are significant contributors to the Birch effect.
72
73 In Mediterranean systems, climate change is predicted to cause increased water stress [18] due
74 to decreased rainfall, extension of the dry season and increased frequency of drying/rewetting
75 cycles, leading to more CO_2 pulses [19, 20]. It has been noted that there is less immediately
76 respirable carbon when the dry season is prolonged [10]. We hypothesized that reduced
77 precipitation in the preceding growing season could affect the response of soil microbial
78 communities to rewetting following the long dry summer. Specifically, we predicted that
79 differences in prior year water input would lead to differences in the biogeochemical toolkit of
80 organisms that grow following wet-up, and that these differences would persist over time.
81 Here, we used stable isotope-informed genome-resolved metagenomics to identify and analyze
82 the genomes of organisms that become active in the week following soil wet-up. From these
83 genomes, we predicted the functional capacities of growing organisms and investigated how
84 they changed over time and due to differences in rainfall history. Our results reveal distinct
85 gene inventories of fast-responding organisms after wet-up in soils that had experienced two
86 distinct rainfall treatments. We document shifts in functional capacities over time, consistent

87 with changes in carbon compound resources, and convergence in the capacities of growing
88 organisms after approximately one week.
89
90 **Results**
91
92 Surface soil samples from a Mediterranean annual grassland with a reduced vs. mean
93 precipitation experiment were collected in the late summer of 2018, prior to the first autumn
94 rainfall event, and used for a ^{18}O-water quantitative stable isotope probing (qSIP) wet-up
95 experiment. DNA was extracted pre-wetup (0h) from soil that experiences mean or reduced
96 precipitation, at 4 time points after water addition from the mean precipitation treatment
97 samples (24h, 48h, 72h and 168h) and 2 time points from the reduced precipitation treatment.
98 The DNA was density fractionated, and 5-7 Gbp of Illumina sequences were acquired per
99 density fraction in addition to 20-28 Gbp from unfractionated DNA per sample. 338
100 dereplicated metagenome assembled genomes (MAGs) were generated from this dataset and
101 combined with 168 MAGs from a previous metagenomic study from a nearby field site sampled
102 during winter [21]. These 503 genomes representing 11 phyla and 23 classes of bacteria and
103 archaea were at least 75% complete. Three additional Firmicutes MAGs, the only
104 representatives of this phylum, were of low quality and therefore used only for abundance and
105 growth analyses. Of the total pool of MAGs, 199 had a breadth (covered fraction) of at least
106 50% in at least one sample from this study. Failure to detect the remainder of the MAGs
107 (304/503) with coverage above this threshold may be because coverage of the genomes in any
108 individual sample was too low to enable assembly (thus they were only reconstructed via co-

109 assembly of data from multiple samples). Short reads mapped to the MAGs made up an
110 average of 12% of total reads per unfractionated sample and 24% of reads from the density
111 fraction samples. This level of assignment of reads to genomes is expected because the
112 majority of DNA from soil originates from very low abundance organisms [22, 23].
113
114 Atom fraction excess (AFE), a metric of growth-based activity, was calculated per MAG based
115 on isopycnic fractionation (fractionation by ultracentrifugation based on changes in DNA
116 density resulting from heavy isotope incorporation, in this case ^{18}O). 79 MAGs had statistically
117 significant isotopic enrichment in at least one time point of one watering regime, as indicated
118 by AFE lower confidence interval limit > 0. We refer to this subset of organisms as growing,
119 since isotope enrichment of DNA requires replication. Hereafter, we distinguish between
120 analyses that include all 506 organisms and analyses of the 199 organisms that were detected
121 by read mapping, of which 79 were growing (sup. table S1).
122
123 We used 16S rRNA based quantitative stable isotope probing (qSIP) to characterize changes in
124 microbial community structure and determine differences in post wet-up mortality in soils that
125 had experienced mean precipitation or reduced precipitation during the previous growing
126 season. We also measured total soil respiration (CO_2) and new plant-biomass derived
127 respiration (i.e., decomposition of carbon fixed during the preceding growing season labeled
128 with ^{13}C). While total soil respiration was not significantly different between the precipitation
129 treatments (fig. 1A), the microbial mortality rate and respiration of newly-fixed plant material

130 were lower in the reduced precipitation treatment (fig 1B, C, p=0.08). The cumulative microbial

131 mortality rate was three orders of magnitude higher in the mean precipitation treatment.

132

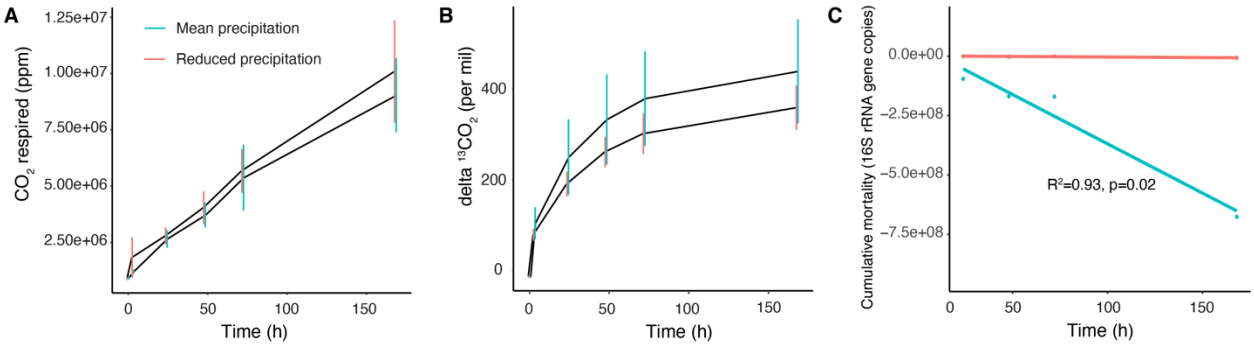

133

134 **Figure 1**: Effects of a 1 week wet-up experiment and two precipitation treatments in annual

135 grassland soils from Hopland, CA: (A) total soil respiration (N=3 per treatment), (B) $^{13}CO_2$

136 respiration of new plant material (N=3 per treatment), (C) cumulative qSIP-based microbial

137 mortality rate, starting at 24h. The linear regression of mortality in the mean precipitation

138 treatment explained 93% of variability with p=0.02. Error bars reflect standard deviation.

139

140 To test whether growing microorganisms were more abundant or became more abundant

141 compared to detected but non-growing organisms we calculated the abundance (measured as

142 reads per kilo million, RPKM) of both growing (N=79) and non-growing (N=121) organisms at

143 each post-wetup time point and in both treatments (fig. 2). Growing microorganisms were

144 significantly more abundant than non-growing organisms at time 0 for both treatments

145 (p<0.001). Abundance of growing or non-growing organisms did not vary between precipitation

146 treatments. There was no statistically significant change in mean abundance over the following

147 week for growing or non-growing microorganisms. With that, the variance in abundance of

148 growing and non-growing organisms in the reduced precipitation treatment decreased

149 significantly over the first 48 hours (fig. 2 see asterisks), indicating that the abundance of the

150 rarer growing organisms increased.

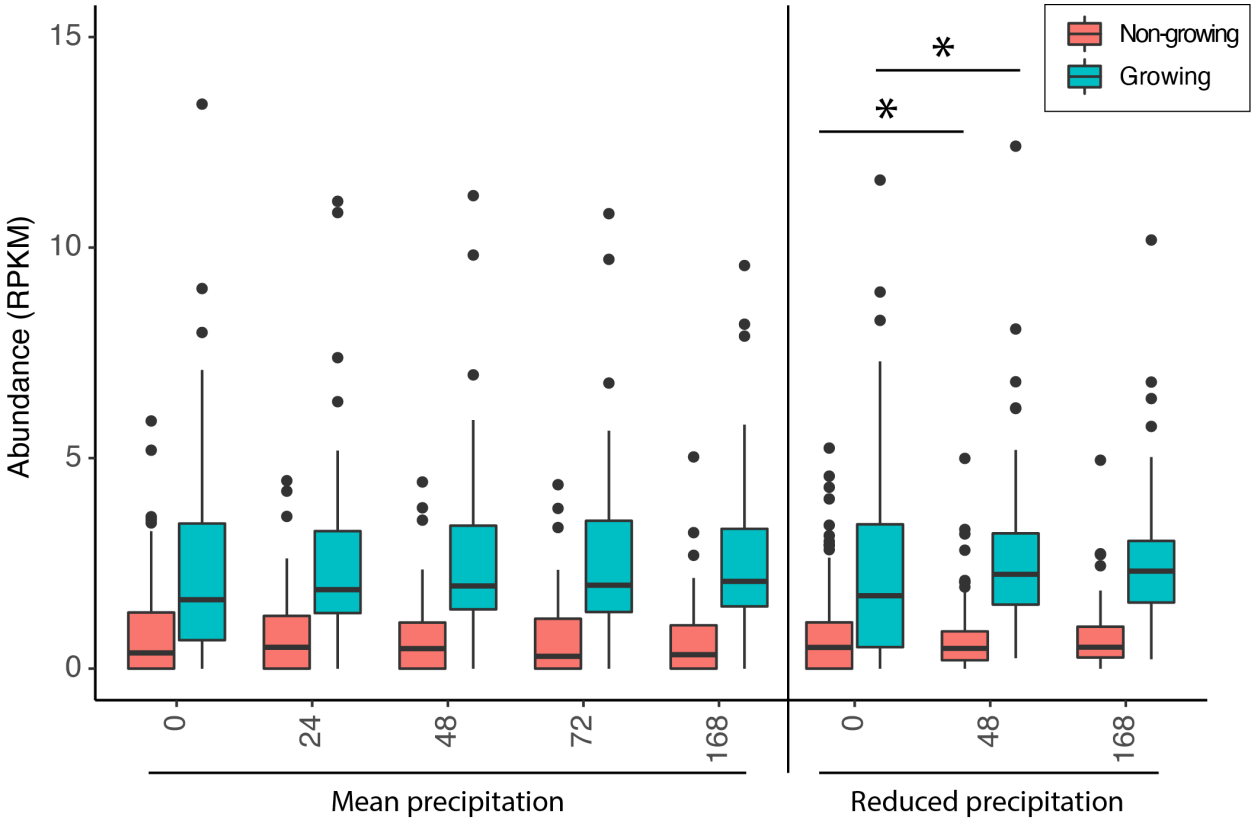

151

152 **Figure 2**: Abundance (RPKM, reads per kilo million) of actively growing versus non-growing

153 bacteria and archaea after a wet-up of dry grassland soils that had experienced mean or

154 reduced precipitation in the preceding growing season. Growth was determined by quantitative

155 stable isotope probing via ^{18}O-water incorporation. All differences between growing organisms

156 (N=79) and not-growing but detected organisms (N=120) are statistically significant ($p<0.001$);

157 within these groups, there are not statistically significant differences with time or precipitation

158 treatment. Boxes represent 75% of that data, whiskers indicate 90%, outliers are denoted by

159 dots. The differences in variance (box length) between 0h and 48h in the reduced precipitation

160 treatment are significant in both growing and not growing organisms ($p<0.05$).

161

162 To test the relationship between abundance and growth, we assessed whether abundant

163 growing organisms were also growing rapidly (AFE > 0.2) by comparing abundances and AFE

164 values of growing microorganisms (N=79) at each time point (fig. 3). Less abundant organisms

165 tended to be fast growing (e.g., Alphaproteobacteria and Gammaproteobacteria) whereas the

166 more abundant organisms were slower growing (e.g., Actinobacteria) over the week post-

167 wetup (linear regression, $p<0.001$, $R^2=0.1$). Significant growth was also detected in

168 Verrucomicrobiae, Gemmatimonadetes, Chloroflexi, Myxococcia, Acidobacteria and the

169 ammonia oxidizing archaea class Nitrososphaeria (fig. 3).

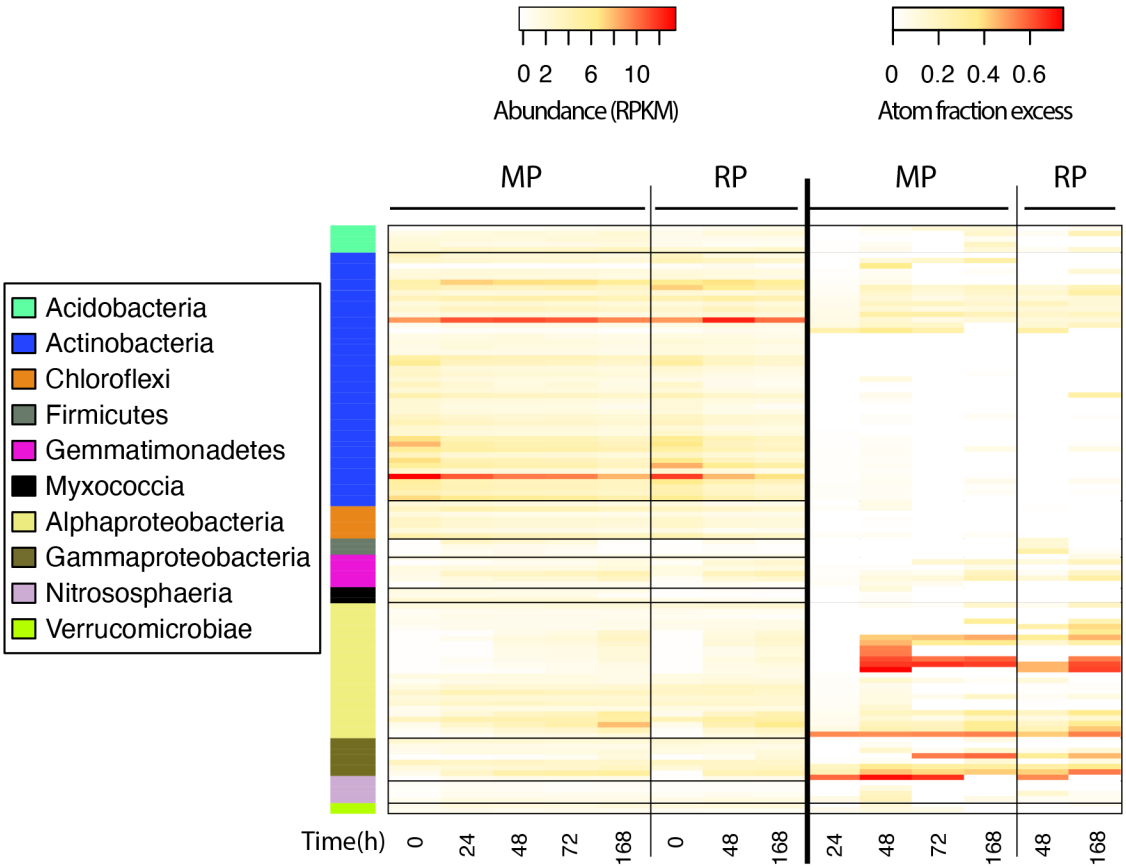

170

171 **Figure 3**: Abundance, enrichment and taxonomic affiliation of 79 taxa that were growing (atom
172 fraction excess confidence interval > 0) after a grassland soil wet-up with ^{18}O enriched water,
173 illustrating that highly abundant organisms in both mean and reduced precipitation treatments
174 were slow growing, and vice versa. Each row represents one taxon, and each column represents
175 one time point. The heat map on the left shows abundance normalized to sample size and MAG
176 length (RPKM) and the heat map on the right shows ^{18}O enrichment (AFE). The rows are
177 ordered by class and enrichment within class, and the left bar represents taxonomy. MP =
178 Mean precipitation, RP = reduced precipitation. Negative AFE values were considered
179 undetectable and converted to zero.
180
181 Most growing organisms were isotopically enriched at multiple consecutive time points, with 63
182 out of 70 and 30 out of 40 in the mean precipitation and reduced precipitation soils respectively
183 (fig. 3). To distinguish boom and bust growth dynamics compared to persistent enrichment on
184 an organism-by-organisms basis, we plotted the number of growing organisms only at one time
185 point vs. in multiple time points (fig. 4). A bloom of 28 newly growing organisms occurred at
186 48h in the mean precipitation treatment, but the majority of these organisms did not continue
187 growing later (see leftmost column in fig. 4), representing boom and bust dynamics. In contrast,
188 for 10 organisms, mostly Proteobacteria, we detected growth in all time points in both
189 treatments (see rightmost column in fig. 4).

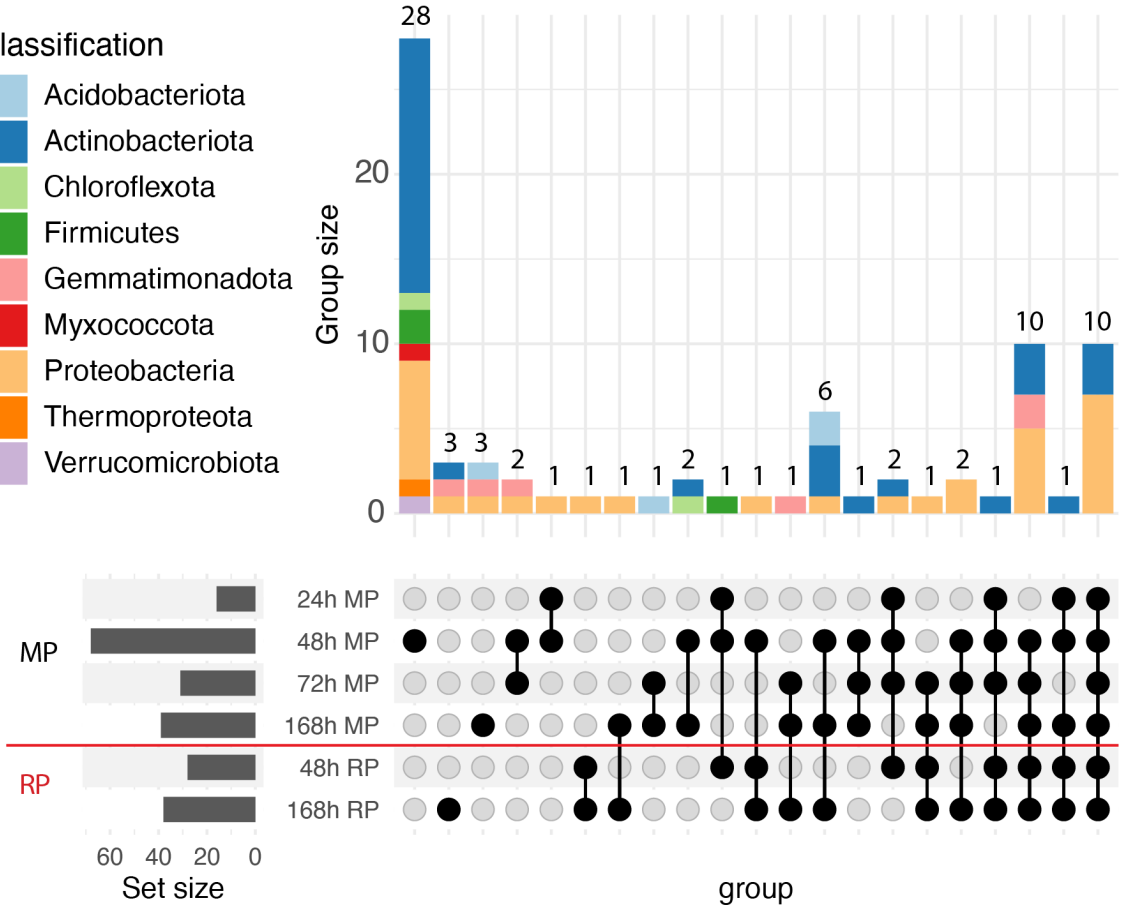

Figure 4: Growth temporal patterns in microbes during the week following wetup of Mediterranean soil that experienced mean or reduced precipitation during the two previous growing seasons. Each row represents a time point in a single precipitation treatment. A single dot per column represents organisms growing only in that time point, whereas linked dots represent organisms growing in both time points/treatments. Each column, denoted by either a single dot or linked dots, represents a group (e.g., organisms that grow at 48h, 72h and 168h in the mean precipitation treatment). Each bar shows how many organisms were growing within a specific group (group size), as well as their taxonomic distribution. In both mean (MP) and reduced precipitation (RP) treatments, when grouped using growth patterns over time (black

200 dots), it is apparent that many organisms grew in just one time point, others displayed a longer
201 boom before bust growth pattern and some grew continuously.
202
203 To probe the extent to which changes in genetic repertoires might underpin shifts in organism
204 abundances we compared the abundances of annotated genes in growing organisms in all
205 samples. The purpose of this gene-centric approach was to identify genes common in growing
206 organisms, as opposed to examining each genome of a growing organism and searching for
207 common genes. We interpret a higher number of genes encoding a trait in growing organisms
208 as an indication of a higher capacity of the community to perform that function. Out of 275,788
209 annotated genes from growing organisms (N=79), the abundance of 30,175 genes changed
210 significantly ($p_{adj} < 0.05$), either between consecutive time points or between treatments at the
211 same time point. In the mean precipitation treatment, the number of genes changing in
212 abundance between consecutive time intervals varied by two to three orders of magnitude.
213 This was not apparent in the reduced precipitation treatments (fig. 5A). However, at time 0h,
214 when comparing the mean vs. reduced precipitation treatments, 11,149 genes were
215 significantly more abundant in one of the treatments (fig. 5B). Most genes at this time point
216 were more abundant in the mean precipitation treatment (sup. fig. 1). This effect waned over
217 time and disappeared completely at 168h (fig. 5A). Ordination of gene abundance in growing
218 organisms revealed progressive temporal changes in community gene abundance in both
219 precipitation treatments (fig. 5C).

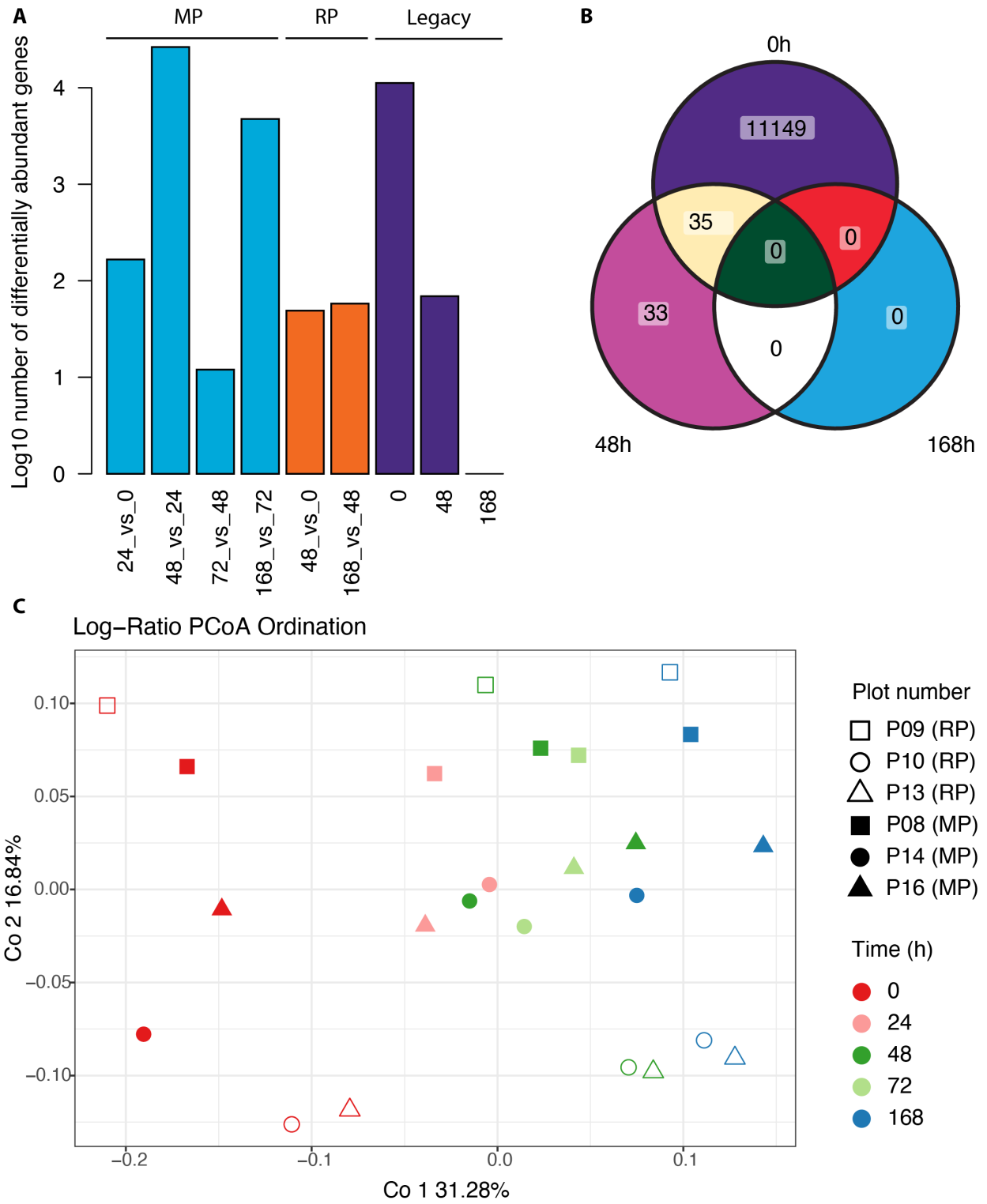

Figure 5: Changes in gene abundance over time and between precipitation treatments reflect changes in abundance of growing organisms after soil wetup. (**A**) Number of significantly

223 (p<0.05) differentially abundant open reading frames (ORFs) at each time point compared to
224 the previous time point (e.g., 48h vs. 24h). Three main comparisons are represented by distinct
225 colors: Mean precipitation treatment (**MP, light blue**), Reduced precipitation treatment (**RP,**
226 **orange**) and comparison between the two at the same time point (**legacy**, **dark purple**). Note
227 that the y axis scale is logarithmic. (**B**) Venn diagram of differentially abundant genes between
228 MP and RP precipitation at the same time point (legacy effect). (**C**) Principal coordinates
229 analysis of log-ratio transformed abundance of genes from growing organisms normalized to
230 sequencing depth (N=79). Shapes represent the location of the field plot from which the
231 metagenome was sequenced: the upper row (plots 8 and 9) or the lower row (plots 10, 13, 14
232 and 16; see methods). Full shapes denote MP, and empty shapes RP. The first two components
233 explain 48% of the variance.
234
235 Dynamics of differentially abundant genes differed for mean and reduced precipitation
236 treatments. In the mean precipitation treatment, the number of differentially abundant genes
237 mostly decreased over the first day, became more abundant over the following day, decreased
238 over the third day and some were more and others less abundant by the end of the week (sup.
239 fig. 1). The reduced precipitation treatment showed a distinct pattern: all differentially
240 abundant genes were more abundant after one week (sup. fig. 1, panel RP 168h vs. 48h).
241 Comparing time points between treatments indicates that most genes were initially (0h) more
242 abundant in the mean precipitation compared to the reduced treatment (sup. fig. 1).
243

244 Within a given treatment, we tested whether the genes that changed in abundance between
245 consecutive time intervals were the same genes. In the mean precipitation treatment, 88% of
246 differentially abundant genes were unique to the 48h time point (sup. fig. 2A). In the reduced
247 precipitation treatment, 99/182 differentially abundant genes were shared between 48h and
248 168h (sup. fig. 2B). Almost all the genes (472/510) that differed at time 48h also differed at 0h
249 (sup. fig. 2C).
250
251 To search for evidence of factors that may have driven changes in growth behavior over time,
252 we evaluated inventories of genes for degradation of carbohydrates, including plant material,
253 fungal material, and other polysaccharides. These functions are performed by carbohydrate
254 active enzymes (CAZy). The difference in abundance patterns of CAZy genes between growing
255 organisms (N=79) and detected but not growing organisms (N=120), i.e., which CAZy genes
256 were more abundant than others, was significant (Wilcoxon rank sum test, $p<0.001$). Thus,
257 organisms that grew during wet-up possessed a different set of CAZy pathways compared to
258 the rest of the bacterial and archaeal community. We looked for a correlation between the
259 number of CAZy genes per genome and atom fraction excess, representing growth. We found
260 that fast growing organisms (AFE>0.2, based on sup. fig. S3) had significantly fewer CAZy genes
261 per genome (average 33 genes per genome), compared to an average of 41 genes per genome
262 in slow growers (sup. fig. 3; one sided Student's t-test, $p=0.02$, $t=-2$). To verify that this
263 difference was not due to lower genome completeness of fast-growing organisms, we
264 compared their genomes completeness values to those of slow-growers and found no
265 significant difference (Student's t-test, $p=0.66$).

266

267 Because complex carbohydrates are an important carbon source in soil not just during wetup
268 but throughout the year, we compared CAZy pathways found in growing organisms to CAZy
269 repertoires of the whole genomically sampled community, defined as all organisms detected in
270 the wetup and during winter (N=503)[21]. We found genes coding for the degradation of
271 rhamnose, pectin, beta mannan, mixed linkage glucans, fucose, chitin, crystalline cellulose more
272 highly represented in growing organisms than in the total set of organisms (sup. fig. 4).

273

274 The total abundance of certain CAZy pathways, especially those related to plant material
275 degradation, changed over time in growing organisms (fig. 6). For example, degradation of
276 amorphous cellulose (C) became relatively more abundant between 24h and 48h. In contrast,
277 xyloglucan (X) degradation became relatively less abundant between 24h and 72h. Based on
278 the percent of growing organisms containing specific CAZy pathways, we observed a functional
279 succession mainly of plant material degrading enzymes. These changes were statistically
280 significant between time points in the mean precipitation treatment, as well as between
281 treatments at 48h, but differences between treatments were not measurable 168h after
282 wetup.

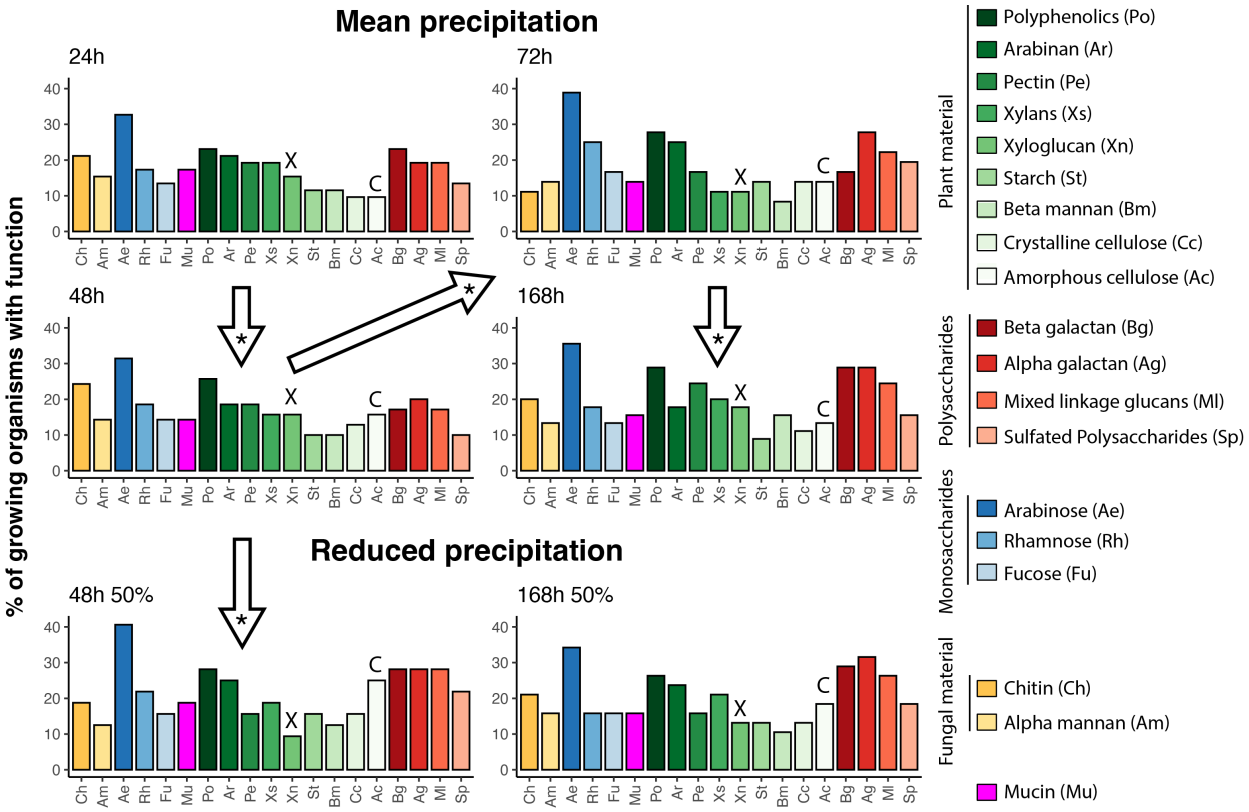

Figure 6: Percent of the organisms that were growing during the week following soil wetup at each time point and contained genes coding for carbohydrate degradation pathways in order of time and precipitation treatment. Arrows indicate significant changes to the entire profile determined by Wilcoxon rank sum test (Benjamini-Hochberg correction for multiple comparisons $p<0.05$). Xyloglucan degradation is marked by an X and Amorphous cellulose by a C above the respective bars.

We also investigated nitrogen acquisition and cycling pathways in growing organisms. Nitrogen in soil exists mostly in the form of large, complex molecules such as proteins, chitin and nucleic acids, but it may also be present as ammonium and other inorganic nitrogen forms [24]. Some inorganic forms of nitrogen can be used as an energy source, such as oxidation of ammonium in

295 nitrification. To investigate what forms of nitrogen growing organisms were taking up or
296 transforming during wet-up, we compared the percentage of growing organisms that contained
297 various nitrogen related genes to the genetic repertoire of the year-round whole community.
298 We found enrichment of genes related to ammonium assimilation and ammonium transporters
299 in growing organisms (Student's paired t-test, $p=0.06$, fig. 7A), but no enrichment of organic
300 nitrogen acquisition genes (Student's paired t-test, $p=0.33$, fig. 7B) except for peptidases
301 (Student's paired t-test, $p=0.1$, fig. 7C). Growing organisms contained more peptidases per
302 genome that belonged mainly to three catalytic groups: metallopeptidases, serine peptidases
303 and cysteine peptidases (fig. 7C). While the number of peptidases per genome in growing
304 organisms did not change over time, there was a significant difference ($p<0.05$) between this
305 number in the mean precipitation treatment at times 48 h and 72 h compared to the reduced
306 precipitation treatment at 48 h.

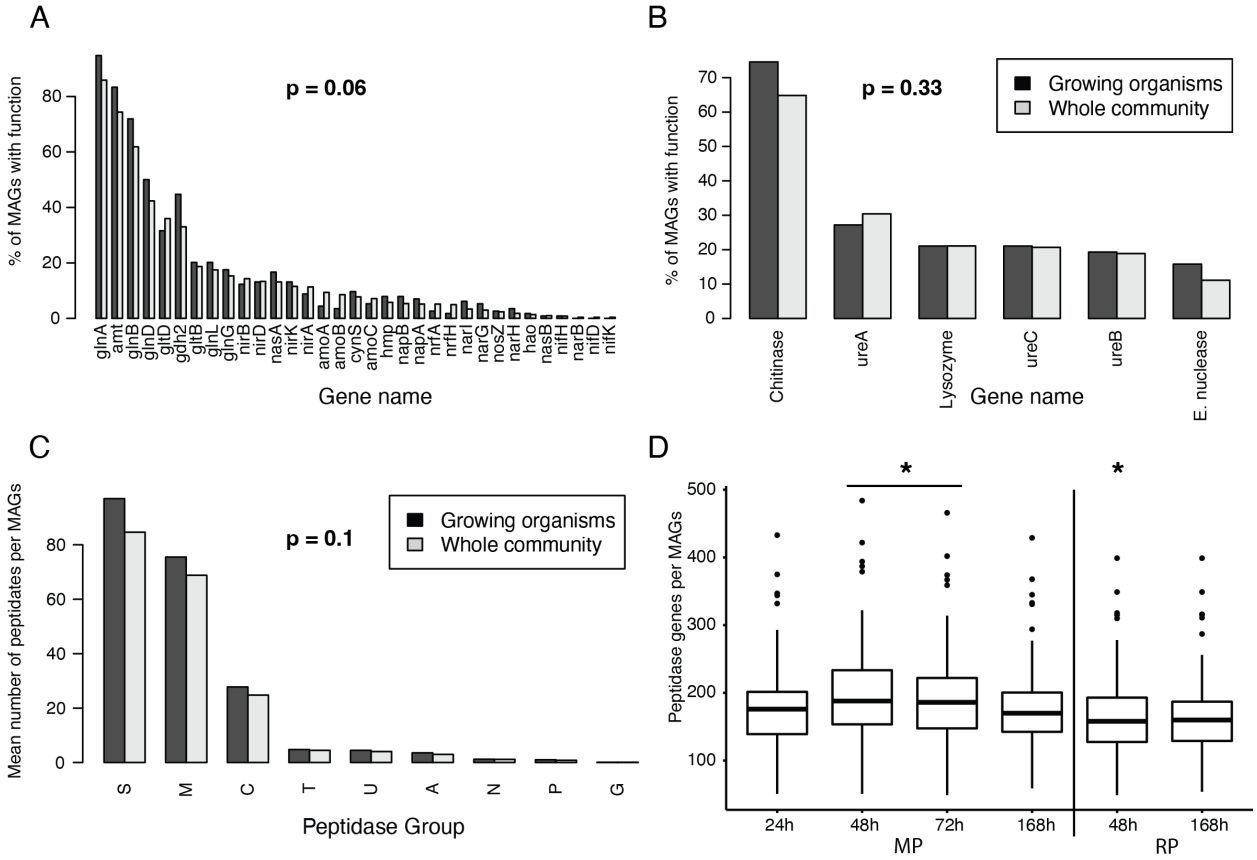

Figure 7: Presence of nitrogen acquisition and cycling traits in growing organisms during the week following soil wetup. Comparison of N acquisition/cycling genes of (A) inorganic N transformations, (B) organic N transformations and (C) catalytic groups of peptidases in growing organisms vs. the whole community. P-values based on Wilcoxon rank sum test are displayed on each panel. Peptidase catalytic groups: S=serine, M=metallo, C=cysteine, T=threonine, U=unknown catalyst, A=aspartic acid, N=asparagine, =mixed, G=glutamic acid. (D) Number of peptidases per organism in growing organisms did not change over time, but the number is significantly ($p<0.05$) lower at 48h in reduced precipitation compared to 48h and 72h at mean annual precipitation, indicated by asterisks. MP = Mean precipitation, RP = reduced precipitation

319 Two of the main strategies in which soil organisms can deal with dry conditions are osmolyte
320 biosynthesis and production of extracellular polysaccharides (EPS) [25]. We searched for genes
321 coding for biosynthesis of the osmolyte trehalose and for EPS synthesis and export. We found
322 significantly more EPS export genes in growing organisms compared to the whole community
323 (Student's paired t-test, p=0.003; fig. 8A) but no significant differences in trehalose synthesis
324 (data not shown). We observed no effect of rainfall treatment or temporal changes in the
325 percent of growing organisms that possess EPS export genes (fig. 8B).

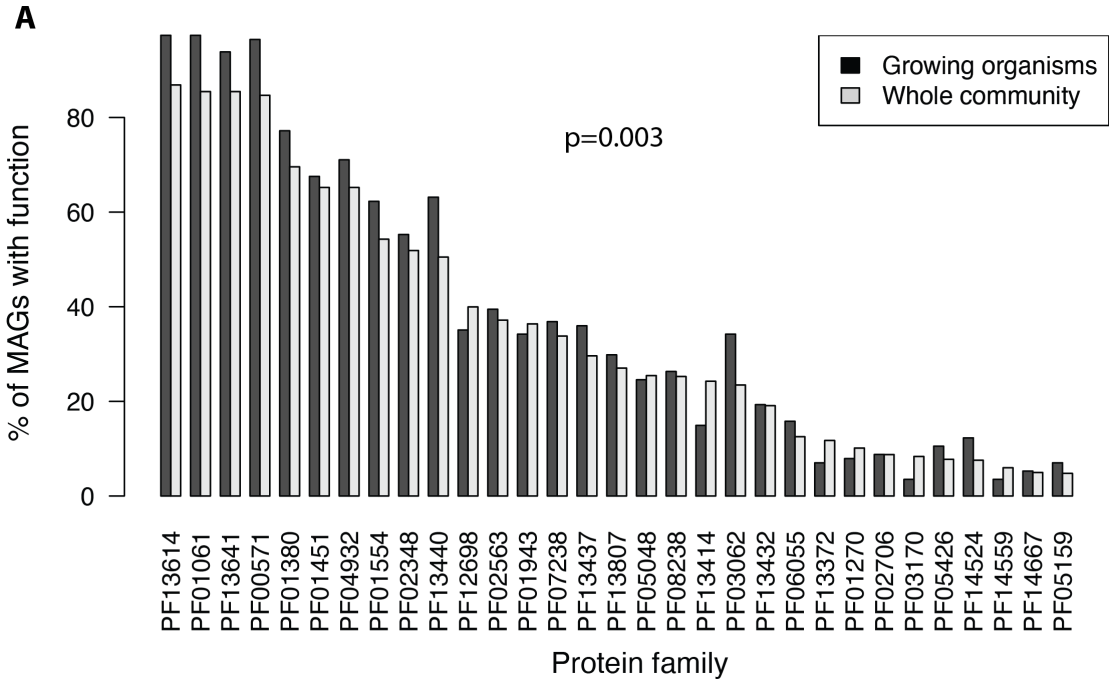

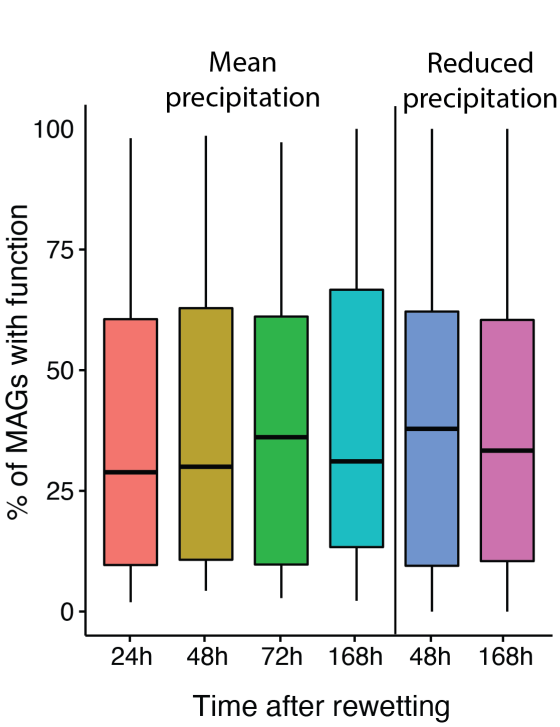

Figure 8: Presence of EPS export genes in metagenome assembled genomes (MAGs) of soil organisms during the week after soil wetup in (A) growing organisms vs. the whole community (Student's paired t-test, p=0.003), and (B) in growing organisms over time (ANOVA, p=0.99).

330 **Discussion**

331

332 We investigated how the history of reduced rainfall impacts the response of soil microbial
333 communities to wet up and the processes by which they acquire nutrients to support growth.
334 While climate change and its associated periodicity of rainfall and longer droughted periods
335 affecting soil moisture are predicted to reduce grassland soil microbial diversity [26], it is the
336 active organisms that determine ecosystem function, therefore we focused on those through
337 stable isotope probing. Integrated results from stable isotope informed genome-resolved
338 metagenomics, gene abundance, and gene function information enabled characterization of
339 the traits of growing organisms that may have contributed to their proliferation during the
340 week following rewetting. Our findings provide a mechanistic foundation for understanding of
341 bulk rate measurements of soil biogeochemical processes following wetup (e.g., respiration).

342

343 As conditions following wetup are quite distinct from those during the summer dry period, we
344 expected that organisms that were abundant during dry down would not be those that grow
345 immediately following wet up. However, in the mean precipitation treatment, the organisms
346 that grew over the week following wetup were a subset of those present in high abundance
347 prior to water addition (t0). Upon wetup, growth was almost certainly primed by newly
348 available labile compounds released by cell death due to osmolysis [17, 25]. Cell lysates may
349 also have been available following desiccation during dry down. Thus, growing organisms may
350 simply be those that utilize compounds released upon cell death rapidly.

351

352 Organisms that grew following wetup were initially more abundant. It may be that they were
353 abundant immediately prior to dry down, or they survived the dry season better than others, or
354 both. We observed a higher prevalence of genes coding for synthesis and export of extracellular
355 polysaccharides in growing organisms compared to the whole community implying that
356 growing organisms may be better poised to survive dry soil conditions. Thus, in combination,
357 we suggest that organisms that were abundant at t0 and grew following wetup were those
358 capable of surviving summer dry conditions and that can grow rapidly on cell lysates. Moreover,
359 organisms that grow may also rely on more complex carbon sources but be primed by labile
360 nitrogen, such as ammonium and amino acids.
361
362 Of the organisms that grew, the fastest growers over the following week were the bacteria that
363 were not the most abundant organisms. Why this is the case remains unclear, but this pattern
364 has been observed previously in grassland soil during the winter [27]. It is possible that
365 organisms that rapidly respond to wetup rely on resources that are less available during most of
366 the year, such as labile carbon and inorganic nitrogen. In support of that, genomes of fast
367 growers contained less carbohydrate degradation genes than those of slow growers, implying a
368 limited toolkit for accessing complex carbon, which is the main carbon source in soil during the
369 rest of the year [28]. A similar pattern of rare and fast-growing bacteria was also identified in a
370 marine environment [29], in which short-lived resource availability was also suggested as a
371 potential mechanism.
372

373 Notably, the organisms that were least abundant prior to wetup exhibited no growth at all
374 following water addition. We suggest that these organisms are part of the low abundance
375 microbial "seed bank" and proliferate under conditions that differ from those studied here.
376 Seed banks are a common strategy of microbial communities to overcome unfavorable
377 conditions and likely underlie successional processes [30]**.** However, we acknowledge that we
378 likely cannot detect growth of all rare organisms due to the noise inherent in qSIP calculations.
379
380 We tracked the changes in gene abundance over the week following wetup and noted that
381 gene abundances changed dramatically and over daily timescales. The observation that genes
382 in growing organisms are almost all becoming less abundant (i.e, regardless of the function of
383 the gene) over the first 24 hr is likely attributed to community-wide mortality during the rapid
384 change in osmotic conditions associated with rewetting of dry soil [7, 8]. Reversal of this
385 pattern over the following day is thus likely attributed to extensive growth across the
386 community.
387
388 Organisms growing at the same time may be using similar resources, and changes in the
389 organisms that are growing could be driven by changes in resources available. Specifically,
390 cellular growth requires acquisition of carbon and nitrogen. The main sources of these
391 elements in soil are organic, i.e., complex carbohydrates and large nitrogen molecules such as
392 proteins, chitin and microbial cell walls. Therefore, we focused on the genetic repertoires
393 related to these substrates and their differential abundances over time and between
394 treatments.

Respiration of $^{13}CO_2$ was produced from labeled plant-derived material, likely a mixture of plant litter and microbial bodies that consumed plant material during the previous year's growing season. It has been previously suggested that in soils that experienced drought, microbes take up less plant derived ^{13}C compounds during the dry season than in soils that didn't experience drought [31]. Therefore, the slightly lower respiration of ^{13}C in the reduced precipitation treatment suggests that microbial bodies served as a carbon source following wetup, and those were less isotopically labeled under reduced precipitation due to the lower uptake of labeled plant material. ^{13}C respiration was detected throughout the week after wetup. However, this respiration was fastest in both treatments within the first 48h, implying usage of ^{13}C-material by fast growers. Fast growing organisms had a smaller number of carbohydrate degrading enzymes than slow growers, implying that fast growth relies on labile carbon in addition to microbial bodies. Thus, based on genetic evidence and respiration of plant-derived C, we suggest that fast growers rely not only on labile C but also on plant-derived material for growth. However, fast growers are likely better competitors for labile carbon, thus necessitating slow growers to specialize in targeting more complex carbon sources.

Importantly, the changing pattern of carbohydrate degrading enzymes over the week-long succession implies reliance on different carbohydrates. Based on succession theory, this would be linked to the changing availability of substrates, which likely drove community composition changes. In contrast, over the same period the vast majority of growing organisms relied on the same nitrogen sources, namely ammonium and extracellular proteins. These could become

417 available following cell death due to osmotic shock at wet-up and continued mortality during
418 the succession. Thus, it appears that the succession we detected is driven more by carbon
419 availability than nitrogen sources.
420
421 Our experimental strategy was designed to test for the effect of reduced precipitation in the
422 prior growing season on microbial growth and propagation of specific functional genes
423 following wetup. We refer to this as a legacy effect. One of the most striking findings of this
424 study is the large magnitude of this effect, reflected in a difference in abundance of thousands
425 of genes at t0 in organisms that grew after wetup. To gain insight into the causes of this legacy
426 effect, we compared the growing microbial populations between precipitation treatments.
427 Reduced precipitation resulted in less detectable growing organisms overall, although unlike
428 previous studies [32] it did not result in lower respiration. Alphaproteobacteria response was
429 altered by precipitation history with a delayed growth response in reduced precipitation as
430 compared to mean annual precipitation. As field conditions were otherwise identical for both
431 treatment groups, the explanation for the delayed response may relate to resource availability.
432 Based on 16S rRNA qSIP, mortality after wet-up in the reduced precipitation treatment was
433 three orders of magnitude lower than in the mean precipitation treatment. The resulting low
434 abundance of labile carbon from cell lysis may have inhibited growth in the first two days,
435 whereas higher mortality in the mean precipitation treatment likely supported growth of new
436 cells. This raises the question of why lysis was less prevalent in the reduced precipitation
437 treatment. While drying and rewetting of soil, even when they result in the same soil moisture,
438 are very different processes [33], they both require the ability to withstand soil moisture

439 changes. Wetup is rapid, and the organisms that survive it must be equipped to handle rapid
440 changes in soil moisture. These same organisms would potentially be those that survived faster
441 drying due to reduced precipitation over the prior year, hence the higher abundance at t0 of
442 organisms that grew following wetup. We suggest that an important driver of the legacy effect
443 was the combination of bacterial resilience to osmotic stress and the resulting decrease in
444 mortality.
445
446 In the soils that experienced reduced precipitation, the carbohydrate degradation gene sets are
447 different compared to gene sets in organisms growing in soils that received mean precipitation.
448 This may point to the availability of different carbohydrates during and after dry-down between
449 the treatment groups. Specifically, a higher fraction of the growing organisms from the reduced
450 precipitation treatment after two days contained genes for degradation of cellulose. Thus, the
451 capacity to degrade cellulose provided a selective advantage following wet up of soils that dried
452 down earlier in the prior year. Further supporting this inference, increased degradation of
453 cellulose was recently shown to be correlated to historical drought [34].
454
455 The legacy effect was surprisingly short-lived, and by the end of the week the metabolic
456 potential of growing microorganisms that previously experienced reduced or mean
457 precipitation converged entirely. This community "reset" could reflect convergence in resource
458 abundance between the treatments, selecting for communities adapted to resource types
459 historically available in this annual grassland. This reset is indicative of a resilient microbial
460 community that converged to be similarly equipped for the next growing season. The intensity

461 of drying/rewetting cycles is predicted to increase with climate change [35]. The experiment
462 conducted here simulated this phenomenon; the results indicate that although the resistance
463 of grassland soil communities to reduced precipitation is not high, their resilience likely is [36].
464
465 **Summary**
466
467 Wet up, a pivotal time point in soils that experience Mediterranean climates, leads to a
468 microbial succession process. Prior studies in Mediterranean soils revealed which organisms
469 grow during this process, but not which traits allow them to do so. The SIP-informed
470 metagenomic data analysis showed that growing organisms are the ones with higher fitness
471 during dry down and have genes for polysaccharide production and export that likely provide
472 resistance to desiccation. We report a disconnect between growth and abundance in organisms
473 that respond to wetup. Slow growers likely rely on complex carbon sources more than fast
474 growers, whereas fast growers are likely better competitors for labile carbon. Finally, we
475 demonstrate a strong but short-lived legacy effect of prior water inputs, with convergence of
476 the sets of growing organisms and their functional traits within a week after wetup.
477
478 **Methods**
479
480 *Field site description*
481 Soil samples for this study were collected from the site of a multi-year precipitation
482 manipulation and $^{13}CO_2$ labeling field experiment (sup. fig. 5)[28] at the University of California

483 Hopland Research and Extension Center (HREC) in Northern California (39° 00′ 14.6″ N, 123° 05′
484 09.1″ W). This region has a Mediterranean climate with cool, wet winters, and hot, dry
485 summers. The HREC field station exists on territory originally home to the indigenous Pomo
486 Nation, and the experiment site is an annual grassland, with naturalized annual grasses such as
487 *Avena spp.* and *Bromus spp.* growing in soil from the Squawrock-Witherell complex. In the Fall,
488 the soil's pH is 7.3 with total C content of 15.1 mg/g and total N of 1.5 mg/g [28].
489 For two years preceding our sample collection, sixteen 3.24 m^2 field plots dominated by
490 *Avena spp.* were watered with either 100% (930 mm) or 50% (465 mm) of the site's mean
491 annual precipitation[28], and in February 2018 plants were isotopically labeled with $^{13}CO_2$ for 5
492 days in the field during the active growing season [28, 37]. Labeled plants and associated soils
493 remained undisturbed in the field throughout the remainder of the growing season and
494 throughout the summer dry season. Samples for the analysis described here were collected on
495 August 28th, 2018, prior to the first rainfall event of the Fall.
496
497 *Sample collection*
498 Topsoil samples (0-15 cm, roughly 0.5 m^3) were collected from six plots, three that had
499 experienced mean annual precipitation and three that experienced 50% precipitation. The soils
500 were collected before the first fall rainfall event, when average soil moisture was 3%, and
501 transferred to the Lawrence Livermore National Laboratory where roots were removed, and
502 soils were homogenized by sieving (2mm) to remove rocks and large plant necromass, all under
503 ambient (hot, dry) conditions.
504

505 *^{18}O-water stable isotope probing*

506 For SIP incubations, 5 g sieved soil from each of the field replicates (*n* = 3) was transferred to a
507 15 ml Nalgene flat bottom vial. One milliliter of isotopically enriched water (98 at% ^{18}O-H_2O) or
508 natural abundance water (as a control) was slowly and evenly pipetted onto the soil and gently
509 mixed with the pipette tip, resulting in a final average gravimetric soil moisture of 22%. After
510 the water addition, vials were immediately sealed inside 500 ml mason jars with lids fitted with
511 septa (to facilitate headspace sampling) and incubated at room temperature in the dark.
512 Parallel jars were destructively harvested at multiple timepoints following the wet-up (0, 24, 48,
513 72, 168 h). At each harvest, vials containing soils were frozen in liquid nitrogen and then stored
514 at -80°C. A total of 66 distinct samples were incubated.

515

516 DNA was extracted from all soil samples using a modified phenol chloroform protocol adapted
517 from Barnard et al. (2015) [38]. Each sample was extracted in triplicate and then replicate DNA
518 extracts were combined. For each extraction, soil (0.4 g +/- 0.001) was added to 2 ml Lysing
519 Matrix E tube (MP Biomedicals) and extracted twice as follows: 500 µl extraction buffer (5%
520 CTAB, 0.5 M NaCl, 240 mM K_2HPO_4, pH 8.0) and 500 µl 25:24:1 phenol:chloroform:isoamyl
521 alcohol were added before shaking (FastPrep24, MP Biomedicals: 30 s, 5.5 m s^{-1}). After
522 centrifugation (16,100 x g, 5 min), residual phenol was removed using pre-spun 2 ml Phase Lock
523 Gel tubes (5 Prime, Gaithersburg, MD, USA) with an equal volume of 24:1 chloroform:isoamyl
524 alcohol, mixed and centrifuged (16,100 x g, 2 min). The aqueous phases from both extractions
525 were pooled, mixed with 7 µl RNAase (10 mg/ml), mixed by inverting, and incubated at 50 °C
526 for 10 min. 335 µL 7.5 M NH_4^+ acetate was added, mixed by inverting, incubated (4 °C, 1 h) and

527 centrifuged (16,100 x g, 15 min). The supernatant was transferred to a new 1.7 ml tube and 1 µl
528 Glycoblue (15 mg/ml) and 1 ml 40% PEG 6000 in 1.6 M NaCl were added, mixed by vortexing,
529 and incubated at room temperature in the dark (2 h). After centrifugation (16,100 x g, 20 min),
530 the pellet was rinsed with 1 ml ice-cold 70% ethanol, air-dried, resuspended in 30 µl 1xTE and
531 stored at -80 °C.
532
533 Samples were density fractionated in a cesium chloride density gradient formed by physical
534 density separation in an ultracentrifuge as previously described (Blazewicz et al. 2020), with
535 minor modifications. For each sample, 5 µg of DNA in 150 µL 1xTE was mixed with 1.00 mL
536 gradient buffer, and 4.60 mL CsCl stock (1.885 g mL^{-1}) with a final average density of 1.730 g mL^{-}
537 ^{1}. Samples were loaded into 5.2 mL ultracentrifuge tubes and spun at 20 ºC for 108 hours at
538 176,284 RCF_{avg} in a Beckman Coulter Optima XE-90 ultracentrifuge using a VTi65.2 rotor.
539 Automated sample fractionation was performed using Lawrence Livermore National
540 Laboratory's high-throughput SIP pipeline 'HT-SIP' [27, 39, 40], which automates fractionation
541 and clean-up tasks for the density gradient SIP protocol. Ultracentrifuge tube contents were
542 fractionated into 36 fractions (~200 µL each) using an Agilent Technologies 1260 isocratic pump
543 delivering water at 0.25 mL min^{-1} through a 25G needle inserted through the top of the
544 ultracentrifuge tube. Each tube was mounted in a Beckman Coulter fraction recovery system
545 with a side port needle inserted through the bottom. The side port needle was routed to an
546 Agilent 1260 Infinity fraction collector. Fractions were collected in 96-well deep well plates. The
547 density of each fraction was then measured using a Reichart AR200 digital refractometer fitted
548 with a prism covering to facilitate measurement from 5 µL, as previously described [41]. DNA in

549 each fraction was purified and concentrated using a Hamilton Microlab Star liquid handling
550 system programmed to automate glycogen/PEG precipitations [40]. Washed DNA pellets were
551 suspended in 40 µL of 1xTE and the DNA concentration of each fraction was quantified using a
552 PicoGreen fluorescence assay. The fractions for each sample were binned into 5 groups based
553 on density (1.6400-1.7039 g/ml, 1.7040-1.7169 g/ml, 1.7170-1.7299 g/ml, 1.7300-1.7449 g/ml,
554 1.450-1.7800 g/ml), and fractions within a binned group were combined and sequenced.
555 Unfractionated DNA from each soil sample was also saved for sequencing.
556
557 *Metagenomic analyses*
558 Biological triplicates of unfractionated DNA from the three field plots, as well as DNA from 5
559 density fractions per sample (n = 234) were sequenced using an Illumina Novaseq S4 2x150bp
560 platform by Novogene Co. (novogene.com). Illumina adapters and phiX sequences were
561 removed using BBmap (https://jgi.doe.gov/data-and-tools/bbtools) and the remaining reads
562 were quality trimmed using Sickle for paired-end reads [42]. This process yielded $155 \cdot 10^6 \pm$
563 $15 \cdot 10^6$ (mean ± standard deviation) reads per unfractionated sample, and $38 \cdot 10^6 \pm 3 \cdot 10^6$ reads
564 per density fraction.
565
566 Triplicates of unfractionated samples from each time point were co-assembled using MEGAHIT
567 version 1.2.9 [43] with presets large-meta and minimum contig length 1000 bp. Reads from
568 unfractionated samples were mapped to each assembly with BBwrap (requiring minimum
569 identity 98%, https://jgi.doe.gov/data-and-tools/bbtools) and used for binning with Maxbin 2.0
570 [44] and MetaBAT2 [45]. Density fractions from each sample were co-assembled and binned in

571 the same manner. Bins from each assembly were refined with the MetaWrap pipeline [46]
572 requiring a minimum of 50% bin completion and maximum 10% bin redundancy. The resulting
573 bins from all assemblies were dereplicated (along with bins assembled from soil samples
574 collected from a nearby site in the winter of 2018 [21]) using dRep [47], requiring 75%
575 completeness and under 10% contamination, yielding 503 unique metagenome assembled
576 genomes (MAGs): 385 from the current study and 193 from the winter study. MAG taxonomy
577 was assigned with the GTDB-tk classify workflow [48]. Three additional low-quality MAGs of
578 Firmicutes were manually binned using ggkbase. These bins were used only for SIP analyses
579 (not for any functional analyses), and were included because a former 16S-rRNA qSIP analysis
580 from the same soil [8] indicated high growth rates of Firmicutes, and we were unable to
581 automatically assemble high quality bins of this phylum.
582
583 Reads from unfractionated samples and density fractions were mapped to our MAG collection
584 described above. Open reading frames (ORFs) were identified in MAGs with Prodigal version
585 2.6.3 [49] and annotated with DRAM [50]. Read counts per ORF from MAGs per sample were
586 parsed with Rsubread [51] and then normalized and analyzed with DESeq2 [52].
587
588 *16S rRNA gene quantification and sequencing*
589 For 16S rRNA gene amplicon sequencing, density fractionated DNA from 330 density fractions
590 was amplified in triplicate 10-uL reactions using primers 515 F and 806 R [53, 54]. Each reaction
591 contained 1uL sample and 9uL of Phusion Hot Start II High Fidelity master mix (Thermo Fisher
592 Scientific) including 1.5mM additional $MgCl_2$. PCR conditions were 95 C for 2 min followed by 20

593 cycles of 95 C for 30 S, 64.5 C for 30 S, and 72 C for 15 S. The triplicate PCR products were then
594 pooled and diluted 10X and used as a template in a subsequent dual indexing reaction that
595 used the same primers including the Illumina flowcell adaptor sequences and 8-nucleotide
596 Golay barcodes (15 cycles identical to initial amplification conditions). Resulting amplicons were
597 purified with AMPure XP magnetic beads (Beckman Coulter) and quantified with a PicoGreen
598 assay on a BioTek Synergy HT plate reader. Samples were pooled at equivalent concentrations,
599 purified with the AMPure XP beads, and quantified using the KAPA Sybr Fast qPCR kit (Kapa
600 Biosciences). Libraries were sequenced on an Illumina MiSeq instrument at Northern Arizona
601 University's Genetics Core Facility using a 300-cycle v2 reagent kit.
602
603 *Quantitative stable isotope probing*
604 Atom fraction excess (AFE), growth rates, mortality rates and net rates were calculated using
605 quantitative stable isotope probing (qSIP) [8, 55] by normalizing MAG relative abundance to the
606 quantity of DNA per density fraction [21]. Relative abundance was calculated with coverM
607 version 0.4.0 (https://github.com/wwood/CoverM), generating read counts (method count) for
608 MAGs with a minimum covered fraction of 50% (method covered_fraction) and dividing by total
609 reads per sample. Cumulative mortality was calculated using mortality rates estimated with 16S
610 rRNA gene sequence and qPCR data as described in Blazewicz et al. 2020 [8, 56].
611
612 *CO_2 Flux quantification*
613 For analysis of CO_2 and $^{13}CO_2$, headspace gas samples (5 ml) were collected at each harvest with
614 a gas-tight syringe and transferred to 20 ml wheaton serum bottles that had been purged and

615 filled with N_2 (1 atm). Total headspace CO_2 was quantified via gas chromotography equipped
616 with a methanizer paired with a flame ionization detector (GC2014, Shimadzu). Carbon isotopic
617 composition ($\delta^{13}C$ relative to the VPDB standard) of CO_2 was measured with a Picarro G2201-i
618 cavity ring down spectrometer fitted with a small sample introduction module (SSIM).
619
620 *Statistical analyses*
621 R code used in this study is available on https://github.com/ellasiera/Wetup_traits.
622 Cumulative mortality regression was calculated with the R base function lm based on mortality
623 values resulting from qSIP analyses. Abundance (RPKM), read counts and breadth (fraction of
624 MAG covered) tables of MAGs per sample were calculated with coverM
625 (https://github.com/wwood/CoverM). For qSIP analyses, counts were converted to zero where
626 breadth was <50%. Relative abundance was then calculated by dividing read counts per MAG
627 by number of reads per sample. Growing organisms *(n* = 79) were defined as MAGs with
628 detected growth for which the lower limit of the confidence interval was greater than zero.
629 Detected organisms *(n* = 200) were those that had breadth >50% and RPKM >0 in at least one
630 sample. Abundance boxplots of growing and non-growing organisms were plotted based on
631 RPKM using ggplot2 [57]. Heatmaps for abundance and median atom fraction excess (AFE) were
632 plotted using the R package heatmap3 [58]. Comparisons of gene abundance between time
633 points and treatments were performed with DESeq2 [52] by defining the variable "condition" to
634 include both time and treatment and comparing all conditions. P values were adjusted for
635 multiple comparisons using FDR correction. Principal coordinates analysis was based on a Bray-

636 Curtis dissimilarity matrix representing gene abundance per sample via the R vegan package
637 [59], and plotted with ggplot2 [57] and ggvenn [60].
638
639 For MAG functional annotation, we used gene annotations from DRAM [50] and
640 determined which MAGs of growing organisms contained CAZy pathways for degradation of
641 carbohydrates in each time point. That number was divided by the number of growing
642 organisms at each time point to get the percent of organisms with the capability to degrade
643 specific substrates. The resulting table was plotted using ggplot2 [57]. Similarly, we analyzed
644 and plotted inorganic and organic nitrogen cycling genes, as well as peptidases. Finally, we used
645 the annotated gene abundances to search for patterns in genes coding for extracellular
646 polysaccharide (EPS) biosynthesis and export, assuming these would be necessary to generate a
647 biofilm.
648
649 **References**

650 1. Placella SA, Brodie EL, Firestone MK. Rainfall-induced carbon dioxide pulses result from sequential
651 resuscitation of phylogenetically clustered microbial groups. *Proc Natl Acad Sci U S A* 2012; **109**:
652 10931–10936.
653 2. Barnard RL, Blazewicz SJ, Firestone MK. Rewetting of soil: Revisiting the origin of soil CO2
654 emissions. *Soil Biol Biochem* 2020; **147**: 107819.
655 3. Xu L, Baldocchi DD, Tang J. How soil moisture, rain pulses, and growth alter the response of
656 ecosystem respiration to temperature. *Global Biogeochem Cycles* 2004; **18**.
657 4. Birch HF. The effect of soil drying on humus decomposition and nitrogen availability. *Plant Soil*

1958; **10**: 9–31.

5. Unger S, Máguas C, Pereira JS, David TS, Werner C. The influence of precipitation pulses on soil respiration--Assessing the 'Birch effect' by stable carbon isotopes. *Soil Biol Biochem* 2010; **42**: 1800–1810.

6. Lee X, Wu H-J, Sigler J, Oishi C, Siccama T. Rapid and transient response of soil respiration to rain. *Glob Chang Biol* 2004; **10**: 1017–1026.

7. Blazewicz SJ, Schwartz E, Firestone MK. Growth and death of bacteria and fungi underlie rainfall-induced carbon dioxide pulses from seasonally dried soil. *Ecology* 2014; **95**: 1162–1172.

8. Blazewicz SJ, Hungate BA, Koch BJ, Nuccio EE, Morrissey E, Brodie EL, et al. Taxon-specific microbial growth and mortality patterns reveal distinct temporal population responses to rewetting in a California grassland soil. *ISME J* 2020; **14**: 1520–1532.

9. Schaeffer SM, Homyak PM, Boot CM, Roux-Michollet D, Schimel JP. Soil carbon and nitrogen dynamics throughout the summer drought in a California annual grassland. *Soil Biol Biochem* 2017; **115**: 54–62.

10. Homyak PM, Blankinship JC, Slessarev EW, Schaeffer SM, Manzoni S, Schimel JP. Effects of altered dry season length and plant inputs on soluble soil carbon. *Ecology* 2018; **99**: 2348–2362.

11. Schimel J, Becerra CA, Blankinship J. Estimating decay dynamics for enzyme activities in soils from different ecosystems. *Soil Biol Biochem* 2017; **114**: 5–11.

12. Kieft TL, Soroker E, Firestone MK. Microbial biomass response to a rapid increase in water potential when dry soil is wetted. *Soil Biology and Biochemistry* . 1987. , **19**: 119–126

13. Kempf B, Bremer E. Uptake and synthesis of compatible solutes as microbial stress responses to high-osmolality environments. *Arch Microbiol* 1998; **170**: 319–330.

14. Halverson LJ, Jones TM, Firestone MK. Release of intracellular solutes by four soil bacteria exposed to dilution stress. *Soil Sci Soc Am J* 2000; **64**: 1630–1637.

682 15. Warren CR. Isotope pool dilution reveals rapid turnover of small quaternary ammonium
683 compounds. *Soil Biol Biochem* 2019; **131**: 90–99.
684 16. Miller AE, Schimel JP, Meixner T, Sickman JO, Melack JM. Episodic rewetting enhances carbon and
685 nitrogen release from chaparral soils. *Soil Biol Biochem* 2005; **37**: 2195–2204.
686 17. Hicks LC, Lin S, Rousk J. Microbial resilience to drying-rewetting is partly driven by selection for
687 quick colonizers. *Soil Biol Biochem* 2022; **167**: 108581.
688 18. Lehner F, Coats S, Stocker TF, Pendergrass AG, Sanderson BM, Raible CC, et al. Projected drought
689 risk in 1.5°C and 2°C warmer climates. *Geophys Res Lett* 2017; **44**: 7419–7428.
690 19. Meisner A, Rousk J, Bååth E. Prolonged drought changes the bacterial growth response to
691 rewetting. *Soil Biology and Biochemistry* . 2015. , **88**: 314–322
692 20. Meisner A, Leizeaga A, Rousk J, Bååth E. Partial drying accelerates bacterial growth recovery to
693 rewetting. *Soil Biol Biochem* 2017; **112**: 269–276.
694 21. Greenlon A, Sieradzki ET, Zablocki O, Koch BJ, Foley MM, Kimbrel JA, et al. Quantitative stable-
695 isotope probing (qSIP) with metagenomics links microbial physiology and activity to soil moisture in
696 Mediterranean-climate grassland ecosystems. *bioRxiv* . 2022. , 2022.05.02.490339
697 22. Pessi IS, Viitamäki S, Virkkala A-M, Eronen-Rasimus E, Delmont TO, Marushchak ME, et al. In-depth
698 characterization of denitrifier communities across different soil ecosystems in the tundra. *bioRxiv* .
699 2022. , 2020.12.21.419267
700 23. Xu L, Dong Z, Chiniquy D, Pierroz G, Deng S, Gao C, et al. Genome-resolved metagenomics reveals
701 role of iron metabolism in drought-induced rhizosphere microbiome dynamics. *Nat Commun* 2021;
702 **12**: 3209.
703 24. Schimel JP, Bennett J. NITROGEN MINERALIZATION: CHALLENGES OF A CHANGING PARADIGM.
704 *Ecology* . 2004. , **85**: 591–602
705 25. Schimel JP. Life in Dry Soils: Effects of Drought on Soil Microbial Communities and Processes. *Annu*

706 *Rev Ecol Evol Syst* 2018.

707 26. Wu L, Zhang Y, Guo X, Ning D, Zhou X, Feng J, et al. Reduction of microbial diversity in grassland soil
708 is driven by long-term climate warming. *Nat Microbiol* 2022.

709 27. Foley MM, Blazewicz SJ, McFarlane KJ, Greenlon A, Hayer M, Kimbrel JA, et al. Active communities
710 and growth of soil microorganisms are framed by mean annual precipitation in three California
711 annual grasslands. *bioRxiv* . 2021. , 2021.12.06.471491

712 28. Fossum C, Estera-Molina KY, Yuan M, Herman DJ, Chu-Jacoby I, Nico PS, et al. Belowground
713 allocation and dynamics of recently fixed plant carbon in a California annual grassland. *Soil Biol*
714 *Biochem* 2022; **165**: 108519.

715 29. Campbell BJ, Yu L, Heidelberg JF, Kirchman DL. Activity of abundant and rare bacteria in a coastal
716 ocean. *Proc Natl Acad Sci U S A* 2011; **108**: 12776–12781.

717 30. Lennon JT, Jones SE. Microbial seed banks: the ecological and evolutionary implications of
718 dormancy. *Nat Rev Microbiol* 2011; **9**: 119–130.

719 31. Fuchslueger L, Bahn M, Hasibeder R, Kienzl S, Fritz K, Schmitt M, et al. Drought history affects
720 grassland plant and microbial carbon turnover during and after a subsequent drought event. *J Ecol*
721 2016; **104**: 1453–1465.

722 32. Göransson H, Godbold DL, Jones DL, Rousk J. Bacterial growth and respiration responses upon
723 rewetting dry forest soils: Impact of drought-legacy. *Soil Biol Biochem* 2013; **57**: 477–486.

724 33. Patel KF, Myers-Pigg A, Bond-Lamberty B, Fansler SJ, Norris CG, McKever SA, et al. Soil carbon
725 dynamics during drying vs. rewetting: Importance of antecedent moisture conditions. *Soil Biol*
726 *Biochem* 2021; **156**: 108165.

727 34. Liu L, Estiarte M, Bengtson P, Li J, Asensio D, Wallander H, et al. Drought legacies on soil respiration
728 and microbial community in a Mediterranean forest soil under different soil moisture and carbon
729 inputs. *Geoderma* 2022; **405**: 115425.

730 35. Dai A, Zhao T, Chen J. Climate Change and Drought: a Precipitation and Evaporation Perspective.
731 *Current Climate Change Reports* 2018; **4**: 301–312.
732 36. Shade A, Peter H, Allison SD, Baho DL, Berga M, Bürgmann H, et al. Fundamentals of microbial
733 community resistance and resilience. *Front Microbiol* 2012; **3**: 417.
734 37. Santos-Medellín C, Estera-Molina K, Yuan M, Pett-Ridge J, Firestone MK, Emerson JB. Spatial
735 turnover of soil viral populations and genotypes overlain by cohesive responses to moisture in
736 grasslands. *bioRxiv* . 2022. , 2022.03.24.485562
737 38. Barnard RL, Osborne CA, Firestone MK. Changing precipitation pattern alters soil microbial
738 community response to wet-up under a Mediterranean-type climate. *ISME J* 2015; **9**: 946–957.
739 39. Trubl G, Kimbrel JA, Liquet-Gonzalez J, Nuccio EE, Weber PK, Pett-Ridge J, et al. Active virus-host
740 interactions at sub-freezing temperatures in Arctic peat soil. *Microbiome* 2021; **9**: 208.
741 40. Nuccio EE, Blazewicz SJ, Lafler M, Campbell AN, Kakouridis A, Kimbrel JA, et al. HT-SIP: A semi-
742 automated Stable Isotope Probing pipeline identifies interactions in the hyphosphere of arbuscular
743 mycorrhizal fungi. *bioRxiv* . 2022. , 2022.07.01.498377
744 41. Buckley DH, Huangyutitham V, Hsu S-F, Nelson TA. Stable Isotope Probing with 15N Achieved by
745 Disentangling the Effects of Genome G+C Content and Isotope Enrichment on DNA Density. *Appl*
746 *Environ Microbiol* 2007; **73**: 3189–3195.
747 42. Joshi NA, Fass J, Others. Sickle: A sliding-window, adaptive, quality-based trimming tool for FastQ
748 files (Version 1.33)[Software]. 2011.
749 43. Li D, Liu C-M, Luo R, Sadakane K, Lam T-W. MEGAHIT: an ultra-fast single-node solution for large
750 and complex metagenomics assembly via succinct de Bruijn graph. *Bioinformatics* 2015; **31**: 1674–
751 1676.
752 44. Wu Y-W, Simmons BA, Singer SW. MaxBin 2.0: an automated binning algorithm to recover genomes
753 from multiple metagenomic datasets. *Bioinformatics* 2016; **32**: 605–607.

754 45. Kang DD, Li F, Kirton E, Thomas A, Egan R, An H, et al. MetaBAT 2: an adaptive binning algorithm for
755 robust and efficient genome reconstruction from metagenome assemblies. *PeerJ* 2019; **7**: e7359.
756 46. Uritskiy GV, DiRuggiero J, Taylor J. MetaWRAP—a flexible pipeline for genome-resolved
757 metagenomic data analysis. *Microbiome* 2018; **6**: 158.
758 47. Olm MR, Brown CT, Brooks B, Banfield JF. dRep: a tool for fast and accurate genomic comparisons
759 that enables improved genome recovery from metagenomes through de-replication. *ISME J* 2017;
760 **11**: 2864–2868.
761 48. Chaumeil P-A, Mussig AJ, Hugenholtz P, Parks DH. GTDB-Tk: a toolkit to classify genomes with the
762 Genome Taxonomy Database. *Bioinformatics* 2019.
763 49. Hyatt D, Chen G-L, Locascio PF, Land ML, Larimer FW, Hauser LJ. Prodigal: prokaryotic gene
764 recognition and translation initiation site identification. *BMC Bioinformatics* 2010; **11**: 119.
765 50. Shaffer M, Borton MA, McGivern BB, Zayed AA, La Rosa SL, Solden LM, et al. DRAM for distilling
766 microbial metabolism to automate the curation of microbiome function. *Nucleic Acids Res* 2020;
767 **48**: 8883–8900.
768 51. Liao Y, Smyth GK, Shi W. The R package Rsubread is easier, faster, cheaper and better for alignment
769 and quantification of RNA sequencing reads. *Nucleic Acids Res* 2019; **47**: e47.
770 52. Love MI, Huber W, Anders S. Moderated estimation of fold change and dispersion for RNA-seq data
771 with DESeq2. *Genome Biol* 2014; **15**: 550.
772 53. Apprill A, McNally S, Parsons R, Weber L. Minor revision to V4 region SSU rRNA 806R gene primer
773 greatly increases detection of SAR11 bacterioplankton. *Aquat Microb Ecol* 2015; **75**: 129–137.
774 54. Parada AE, Needham DM, Fuhrman JA. Every base matters: assessing small subunit rRNA primers
775 for marine microbiomes with mock communities, time series and global field samples. *Environ
776 Microbiol* 2016; **18**: 1403–1414.
777 55. Hungate BA, Mau RL, Schwartz E, Caporaso JG, Dijkstra P, van Gestel N, et al. Quantitative microbial

778 ecology through stable isotope probing. *Appl Environ Microbiol* 2015; **81**: 7570–7581.

779 56. Koch BJ, McHugh TA, Hayer M, Schwartz E, Blazewicz SJ, Dijkstra P, et al. Estimating taxon-specific

780 population dynamics in diverse microbial communities. *Ecosphere* . 2018. , **9**

781 57. Wickham H. ggplot2: Elegant Graphics for Data Analysis. 2016. Springer.

782 58. Zhao S, Guo Y, Sheng Q, Shyr Y. Heatmap3: an improved heatmap package with more powerful and

783 convenient features. *BMC Bioinformatics* 2014; **15**: P16.

784 59. Oksanen J, Kindt R, Legendre P, O'Hara B, Simpson GL, Solymos P, et al. The vegan package.

785 *Community ecology package [http://r-forge r-project org/projects/vegan/]* 2008.

786 60. Yan. ggvenn: Draw Venn Diagram by 'ggplot2'. *R Package Version* .

787

788 **Acknowledgements**

789

790 The authors thank members of the Firestone and Pett-Ridge groups who helped with field

791 sampling and soil processing, Shufei Lei and Rohan Sachdeva for bioinformatic support, Max Li

792 for help with the soil incubations and DNA extractions, Ryan Gini for help with GC analyses,

793 Michaela Hayer for help with qPCR and amplicon sequencing, and Marissa Lafler for operation

794 of the LLNL HT-SIP qSIP pipeline and the Picarro CRDS.

795 This research was supported by the U.S. Department of Energy (DOE), Office of Biological and

796 Environmental Research (BER), Genomic Science Program Lawrence Livermore National

797 Laboratory (LLNL) 'Microbes Persist' Soil Microbiome Scientific Focus Area SCW1632, and a

798 subaward to UC Berkeley. Field plots, the precipitation experiment and the $^{13}CO_2$ labeling study

799 were initially generated via DOE BER awards DE-SC0020163 and DE-SC0016247 (to MKF) and

awards SCW1589, and SCW1421 (to JPR); designed and maintained by Dr. Mengting Yuan, Dr. Donald Herman, Katerina Estera-Molina, and staff of the Hopland Research and Extension Center (HREC) through the University of California Division of Agriculture and Natural Resources. Work at LLNL was performed under the auspices of the Department of Energy, Contract DE-AC52-07NA27344.

Ethics approval and consent to participate

Not applicable

Consent for publication

Not applicable

Availability of data and material

All raw data used in this publication is available on the NCBI short read archive under BioProject PRJNA856348. No custom tools were used to analyze the data.

Competing interests

The authors declare that they have no competing interests.

Funding

This research was supported by the U.S. Department of Energy (DOE), Office of Biological and Environmental Research (BER), Genomic Science Program Lawrence Livermore National

Laboratory (LLNL) 'Microbes Persist' Soil Microbiome Scientific Focus Area SCW1632, and a subaward to UC Berkeley. Field plots and precipitation management were initially generated via DOE BER awards DE-SC0020163 and DE-SC0016247 (to MKF) and awards SCW1589, and SCW1421 (to JPR).

Authors' contributions

ETS performed all bioinformatics and statistical analyses on metagenomic data, wrote and revised the manuscript.

AG provided genomic sequences, participated in sample processing and provided input on the manuscript.

AMN assisted with graphical illustrations and provided feedback on the manuscript.

MKF advised on paper writing and analyses and provided funding for the original precipitation manipulation experiment.

JPR co-designed the experiment, provided equipment and funding, processed samples, provided feedback and revised the paper.

SJB co-designed and ran the experiment, advised on the paper, participated in writing and analyzed 16S-qSIP data.

JFB advised and participated in paper writing and analyses.